



# Determination of phase relations of the olivine–ahrensite transition in the $\text{Mg}_2\text{SiO}_4$ – $\text{Fe}_2\text{SiO}_4$ system at 1740 K using modern multi-anvil techniques

Artem Chanyshv<sup>1,2</sup> · Dmitry Bondar<sup>2</sup> · Hongzhan Fei<sup>2</sup> · Narangoo Purevjav<sup>2</sup> · Takayuki Ishii<sup>2,3</sup> · Keisuke Nishida<sup>2</sup> · Shrikant Bhat<sup>1</sup> · Robert Farla<sup>1</sup> · Tomoo Katsura<sup>2,3</sup>

Received: 31 March 2021 / Accepted: 11 August 2021 / Published online: 20 September 2021  
© The Author(s) 2021

## Abstract

The phase relations of iron-rich olivine and its high-pressure polymorphs are important for planetary science and meteoritics because these minerals are the main constituents of terrestrial mantles and meteorites. The olivine–ahrensite binary loop was previously determined by thermochemical calculations in combination with high-pressure experiments; however, the transition pressures contained significant uncertainties. Here we determined the binary loop of the olivine–ahrensite transition in the  $(\text{Mg,Fe})_2\text{SiO}_4$  system at 1740 K in the pressure range of 7.5–11.2 GPa using a multi-anvil apparatus with the pressure determined using in situ X-ray diffraction, compositional analysis of quenched run products, and thermochemical calculation. Based on the determined binary loop, a user-friendly software was developed to calculate pressure from the coexisting olivine and ahrensite compositions. The software is used to estimate the shock conditions of several L6-type chondrites. The obtained olivine–ahrensite phase relations can also be applied for precise in-house multi-anvil pressure calibration at high temperatures.

**Keywords** Experimental · Olivine · Ahrensite · Phase transition · Thermobarometry · Meteorites

## Introduction

Fe-rich olivine could be an important constituent of the mantles of oxidized terrestrial planets. Although olivine in the Earth's uppermost mantle is considered to have  $\text{Mg}\# = \text{Mg}/(\text{Mg} + \text{Fe}^{2+}) = 0.9$ , olivine in the Martian mantle likely has  $\text{Mg}\# = 0.75$  (Khan et al. 2018). The composition of more distant terrestrial planets can be estimated from the composition of CI chondrites (McDonough and Sun 1995), and assuming that all Fe is present in their mantles as  $\text{Fe}^{2+}$ , their upper mantles would be composed of olivine with  $\text{Mg}\# = 0.55$ .

This theory is supported by a recent spectroscopy study that revealed that the surfaces of some asteroids are dominated by Fe-rich olivine ranging from  $\text{Mg}\# = 0.55$ – $0.76$  (Sanchez et al. 2014). The phase relations of olivine and its high-pressure polymorphs in intermediate to Fe-rich compositions are, therefore, significant for understanding the structure and dynamics of oxidized terrestrial planets.

Olivine ( $\alpha$ - $(\text{Mg,Fe})_2\text{SiO}_4$ ) is well known to transform to a polymorph with the spinel structure ( $\gamma$ - $(\text{Mg,Fe})_2\text{SiO}_4$ ) at high pressure (Ringwood 1958). This polymorph with  $\text{Mg}_2\text{SiO}_4$  composition has been named ringwoodite (Binns et al. 1969). Later, a Fe-rich polymorph with  $\text{Mg}\# = 46$  has been found in a shocked meteorite and named ahrensite (Ma et al. 2016). Hereafter we will call the  $\alpha$ - and  $\gamma$ - $(\text{Mg,Fe})_2\text{SiO}_4$  with more or equal to 50 mol%  $\text{Mg}_2\text{SiO}_4$  as forsterite and ringwoodite, respectively, whereas  $\alpha$ - and  $\gamma$ - $(\text{Mg,Fe})_2\text{SiO}_4$  with less than 50 mol%  $\text{Mg}_2\text{SiO}_4$  as fayalite and ahrensite, respectively. Both ringwoodite and ahrensite in meteorites formed from the host olivine via a solid-state transformation.

Communicated by Timothy L. Grove.

✉ Artem Chanyshv  
artem.chanyshv@uni-bayreuth.de

<sup>1</sup> Deutsches Elektronen-Synchrotron DESY, Notkestr. 85, 22607 Hamburg, Germany

<sup>2</sup> Bayerisches Geoinstitut (BGI), University of Bayreuth, 95440 Bayreuth, Germany

<sup>3</sup> Center for High Pressure Science and Technology Advanced Research (HPSTAR), Beijing 100094, China

The phase relations of the olivine–ahrensite transition<sup>1</sup> are, therefore, vital to estimate shock conditions of meteorite impacts.

The determination of olivine–ahrensite phase relations in the  $(\text{Mg,Fe})_2\text{SiO}_4$  system is valuable not only for planetary science but also for high-pressure technology. The pressure in a multi-anvil press is estimated using an in-house pressure calibration curve against the press load. Calibration curves at ambient temperature below 10 GPa are usually constructed by detecting the resistance changes of metals (e.g. Bi, Ba) associated with their high-pressure phase transitions, for which only one run is necessary. To construct a calibration curve at high temperature, mineral phase transitions, such as the quartz–coesite–stishovite transitions in  $\text{SiO}_2$  (Mirwald and Massonne 1980; Ono et al. 2017) and fayalite–ahrensite transition in pure  $\text{Fe}_2\text{SiO}_4$  (Yagi et al. 1987), must be bracketed by repeatedly conducting runs with variable press loads. Using olivine solid solutions, it is possible to precisely determine the pressure in a single run based on Mg# measurements of coexisting olivine and ahrensite. For this approach, an accurate phase diagram of olivine–ahrensite is required.

Despite its importance, the phase relations of the olivine–ahrensite transition remain poorly constrained. This question was experimentally investigated more than half a century ago by Akimoto and Fujisawa (1968) using the quench method with a tetrahedral multi-anvil press, where pressure was calibrated only at ambient temperature. The phase relations were later studied mainly by thermochemistry. Akaogi et al. (1989) constructed a phase diagram of this transition based on high-temperature solution calorimetry results. Although the transition pressure values of the  $\text{Fe}_2\text{SiO}_4$  end-member were fixed based on those determined by high  $P$ – $T$  in situ X-ray diffraction experiments (Yagi et al. 1987), the transition pressure of the  $\text{Mg}_2\text{SiO}_4$  end-member cannot be experimentally determined due to the stability of wadsleyite. Phase relations in the Mg-rich side of the loop may, therefore, contain significant uncertainties. Indeed, Frost (2003) built a phase diagram using the same calculation procedures as Akaogi et al. (1989), but applied different interaction parameters obtained experimentally at high pressure, and his thermochemically constructed binary loop differed significantly from the experimental data. Because the compositions of coexisting olivine and ahrensite were determined reliably in Frost (2003), one can suggest that the thermochemical calculation of the olivine–ahrensite loop does not provide valid data, especially for the Mg-rich side of the loop. The olivine–ahrensite transition should, therefore, be determined using modern high-pressure experimental techniques.

In this study, we determined the binary loop of the olivine–ahrensite transition in the  $\text{Mg}_2\text{SiO}_4$ – $\text{Fe}_2\text{SiO}_4$  system at a temperature of 1740 K using the multi-anvil technique with the pressure determined using in situ X-ray diffraction (XRD), compositional analysis of quenched run products by electron microprobe, and thermochemical calculation. Using obtained data, we developed software to calculate pressure from the compositions of olivine and ahrensite. The shock conditions of several meteorites were estimated using the ahrensite compositions.

## Experimental procedure

### Sample preparation

Olivine solid solutions  $(\text{Mg}_x\text{Fe}_{1-x})_2\text{SiO}_4$  with  $x=0.1, 0.2, 0.3, 0.4, 0.6,$  and  $0.8$ , which are named Fo10, Fo20, Fo30, Fo40, Fo60, and Fo80, respectively, were used as the starting materials. Fo10, Fo20, Fo30, and Fo40 were prepared from reagent grade oxides of  $\text{SiO}_2$ ,  $\text{MgO}$ , and  $\text{Fe}_2\text{O}_3$ .  $\text{SiO}_2$  and  $\text{MgO}$  were heated at 1270 K, and  $\text{Fe}_2\text{O}_3$  at 770 K for 16 h to remove adsorbed water. The powders were stored in a vacuum furnace at 370 K overnight before weighing, mixed in proportions corresponding to Fo10, Fo20, Fo30, and Fo40, and ground with acetone in an agate mortar for 1 h. The resulting mixtures were compressed into pellets and then sintered for 20 h in a  $\text{CO}$ – $\text{CO}_2$  gas-mixing furnace at temperatures of 1370–1420 K and an oxygen partial pressure ( $f\text{O}_2$ ) of approximately 1–2 log unit above the iron-wustite (IW) buffer. The pellet color changed from rose to grey indicating a change from  $\text{Fe}^{3+}$  to  $\text{Fe}^{2+}$ . This procedure was repeated 2–4 times for each composition until no phases other than olivine were confirmed based on their powder XRD patterns, which were obtained using a micro-focused X-ray diffractometer (Bruker AXS Discover 8) with a two-dimensional solid-state detector (VANTEC500) and micro-focus source ( $\text{I}\mu\text{S}$ ) with  $\text{Co-K}\alpha$  radiation operated at 40 kV and 500  $\mu\text{A}$ . Fo60 and Fo80 were prepared by the sol–gel method (Ishii et al. 2018, 2019). Mg and Fe solutions were separately dissolved in a mixture of  $\text{HNO}_3$ , pure water, and tetraethylorthosilicate  $(\text{CH}_3\text{CH}_2\text{O})_4\text{Si}$ , and then mixed in the desired molar ratios of Mg:Fe:Si. Ammonia was added to the solutions to make gels, which were then heated stepwise to 1700 K. The recovered powders were heated at 1500 K for 12 h in a  $\text{CO}$ – $\text{CO}_2$  gas-mixing furnace controlled at an  $f\text{O}_2$  of  $\sim 1$  log unit above the IW buffer. The XRD patterns of the recovered samples showed olivine with a trace amount of enstatite. Disks with a diameter of 1 mm and height of 0.3 mm were then prepared from the sintered olivine solid solutions.

<sup>1</sup> For simplicity, we will call forsterite–fayalite–ringwoodite–ahrensite transition as olivine–ahrensite phase transition.

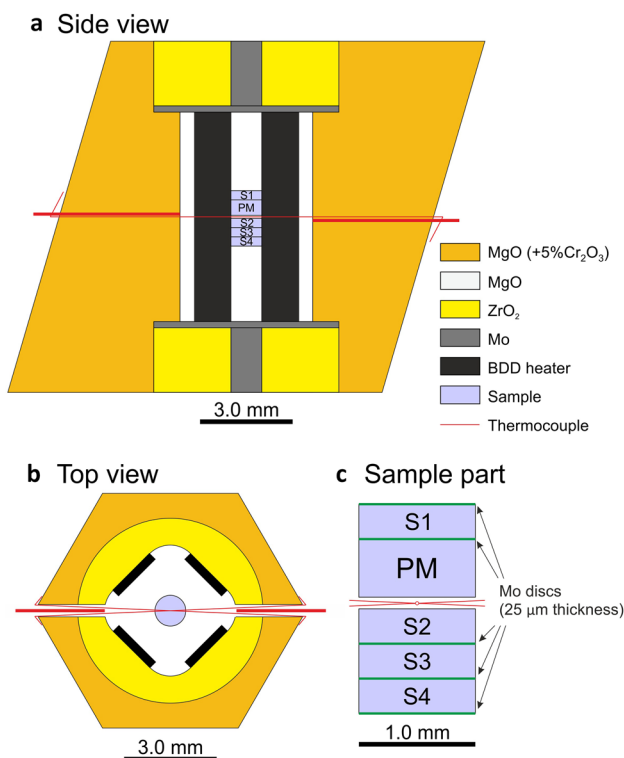


**Fig. 1** Schematic drawing of a cell assembly used in the 3×5 MN six-axis multi-anvil apparatus (TEL 8 mm): side view (a), top view (b), and enlarged sample part from the side view (c). S1–S4 sample positions. *PM* pressure marker (sintered MgO)

### In situ X-ray diffraction

High-pressure experiments were conducted using the 3×5 MN six-axis multi-anvil press at the P61B beamline at the Deutsches Elektronen-Synchrotron (DESY) in Hamburg. This apparatus is equipped with an energy-dispersive XRD system, a Ge solid-state detector (SSD) with a 4096 multi-channel analyzer (MCA) and CCD camera for radiographic imaging. An energy range of the SSD-MCA was calibrated using the gamma-ray lines of different metals prior to the measurements. The diffraction angle ( $2\theta$ ) was calibrated before each experiment with a precision of  $0.0001^\circ$  using the XRD pattern of MgO at ambient pressure as a standard.

We used a modified high-pressure cell assembly described in Nishida et al. (2020). The experimental cell consisted of an MgO+Cr<sub>2</sub>O<sub>3</sub> octahedral pressure medium, strip-type boron-doped diamond (BDD) heater, tetragonal MgO prism with round corners, ZrO<sub>2</sub> thermo-insulators, and Mo electrodes (Fig. 1). Disk-shaped samples and MgO pressure marker were located in the center of the MgO prism and isolated from one another by Mo disks (0.025 mm). The sample and pressure-marker disks were 0.3 and 0.5 mm in thickness, respectively. Typically, we loaded four samples (S1, S2, S3, and S4) with different compositions in one run

(Fig. 1c). In one experiment, a disk of S1 was replaced by an additional MgO disk. The temperature was measured using a W<sub>97</sub>Re<sub>3</sub>–W<sub>75</sub>Re<sub>25</sub> thermocouple located at the center of the furnace between the MgO and sample (S2) disks. Sample S2 was selected in each run, so that its composition fell into the olivine–ahrensite coexistence loop under our target conditions (Akaogi et al. 1989). The thermocouple was electrically isolated from the BDD stripes with the MgO prism.

The cell assembly was compressed to the desired press load and then heated to 1700 K. At this temperature, the sample pressure was carefully monitored every 50–100 s and held constant by increasing the press load to compensate for pressure drop due to plastic material flow at high temperature (Ishii et al. 2018, 2019). Temperature fluctuations were limited to  $\pm 3.0$  K. After 20 min at 1700 K, the sample was quenched and analyzed by XRD prior to decompression. The pressure effect of the thermoelectromotive force of the thermocouple was corrected using the equations determined by Nishihara et al. (2020) after the experiments, with recalculated temperatures of 1732.6–1748.0 K (Table 1). For the phase diagram construction and thermochemical calculation, we averaged these values as 1740 K.

An incident X-ray beam collimated to dimensions of 50  $\mu\text{m}$  horizontally and 300  $\mu\text{m}$  vertically was directed at the sample through the gaps between the second stage anvils. All experiments were carried out with the press oscillating around the vertical press axis between  $0^\circ$  and  $4^\circ$  during the XRD measurement to suppress intensity heterogeneities of the diffracted peaks. The pressure was calculated from the MgO unit cell volumes using the equations of state proposed by Tange et al. (2009) and the pressure-corrected temperatures based on the third-order Birch–Murnaghan and Vinet equations of state. To calculate the MgO unit cell volumes, we used seven diffraction peaks (111, 200, 220, 222, 400, 420, and 422), which allow precise pressure determination (Ishii et al. 2018, 2019).

### Sample analyses

The recovered run products were polished and investigated using a scanning electron microscope (SEM) with a back-scattering detector and acceleration voltage of 20 kV to observe two phases with (Mg + Fe):Si = 2:1 stoichiometry but different Fe/(Mg + Fe) ratios and take high-resolution images (Fig. 2).

The chemical compositions of olivine and ahenrite were analyzed using a JEOL JXA-8200 electron probe microanalyzer (EPMA) equipped with five wavelength-dispersive spectrometers (WDS). The samples were analyzed with a point-beam using an acceleration voltage of 15 kV, probe current of 15 nA, and counting time of 20 s on the peak and 10 s on the two background positions at both sides of the peak. Measured peak counts were corrected using the PRZ

**Table 1** Experimental conditions and composition of run products obtained by EPMA

Run. No.	T (K) before P-correction of EMP	T (K) after P-correction of EMF	P (GPa) before T-correction	P (GPa) after T-correction	Starting material	Sample position	Composition of olivine ( $X_{\text{Mg},\text{SiO}_4}^{\text{Ol}}$ )	Composition of ahrensite ( $X_{\text{Mg},\text{SiO}_4}^{\text{Ahr}}$ )	Olivine molar volume <sup>b</sup> (cm <sup>3</sup> / mol)	Ahrensite molar volume <sup>b</sup> (cm <sup>3</sup> / mol)
									$V_{\text{Mg}_2\text{SiO}_4}^{\text{Ol}}$	$V_{\text{Mg}_2\text{SiO}_4}^{\text{Ahr}}$
HH309 <sup>a</sup>	1701.0 (3.0)	1748.0 (3.0)	12.19 (17)	12.49 (17)	Fo80	S1	0.874 (12)		41.60	44.29
HH310	1701.1 (1.1)	1744.6 (1.1)	10.91 (17)	11.19 (17)	Fo60	S2	0.773 (16)	0.518 (1)	42.00	44.67
HH300	1701.7 (2.4)	1743.4 (2.4)	10.08 (12)	10.34 (11)	Fo60	S2	0.699 (11)	0.416 (10)	42.28	44.92
HH311	1699.8 (1.0)	1737.9 (1.0)	8.94 (14)	9.18 (14)	Fo40	S2	0.572 (7)	0.304 (4)	42.67	45.29
HH312	1700.4 (9)	1735.3 (9)	8.03 (13)	8.25 (13)	Fo30	S2	0.447 (4)	0.218 (6)	43.00	45.59
HH314	1700.4 (6)	1732.6 (6)	7.28 (13)	7.48 (13)	Fo20	S2	0.295 (7)	0.122 (2)	43.28	45.86

The molar volumes of the olivine and ahrensite endmembers from previous studies recalculated to our experimental conditions are also included, which are used for the thermodynamic calculations of reactions (1) and (2).

<sup>a</sup>The run product appears as the coexistence of olivine and wadsleyite and was, therefore, not used for thermodynamic calculations

<sup>b</sup>The endmember molar volumes are from previous studies (Katsura et al. 2004, 2009; Jacobs et al. 2001) recalculated to 1740 K and the experimental pressure conditions using their reported parameters of thermal expansion coefficients and Birch–Murnaghan equations of state

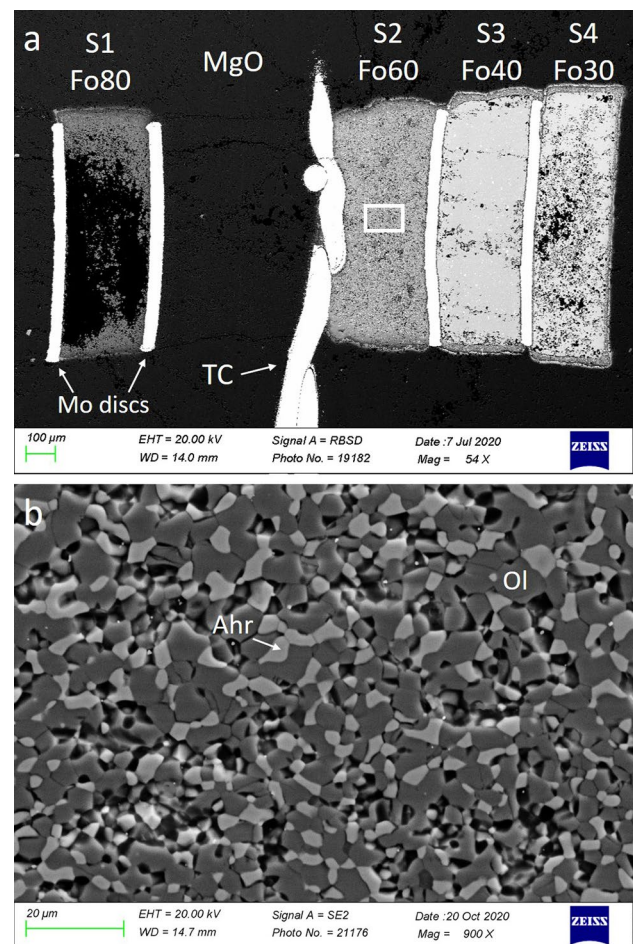


**Fig. 2** SEM images of run products from experiment HH300 at 10.34 (11) GPa and 1743.4 (24) K. **a** Overview of the cross-section of all samples separated with Mo discs. TC—W<sub>97</sub>Re<sub>3</sub>–W<sub>75</sub>Re<sub>25</sub> thermocouple. **b** Enlarged image of sample S2 (white square in **a**)

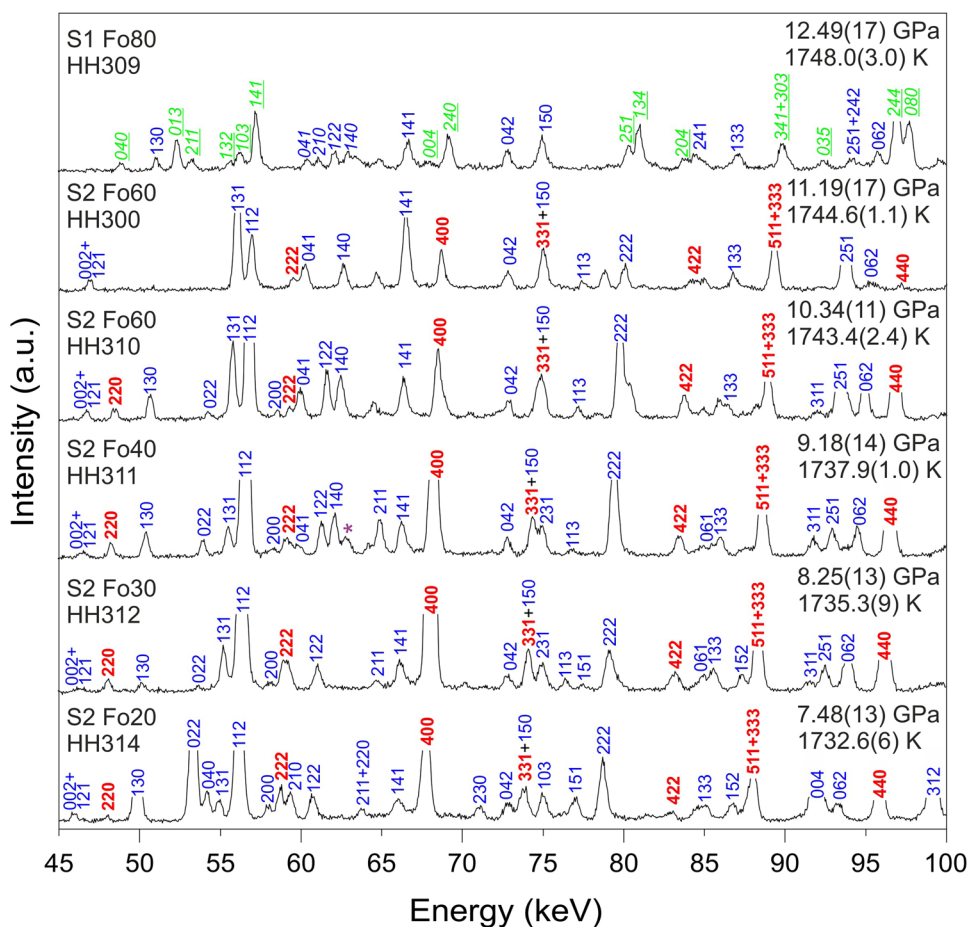
(Phi–Rho–Z) method (Armstrong 1991). An enstatite single crystal was used as the standard for Mg and Si, and metallic Fe was used for Fe. Oxygen was calculated by stoichiometry. To obtain good statistics, 11–41 measurements were collected for each phase from every run.

## Results and discussion

### Run products analyses

The XRD analyses revealed the coexistence of  $\alpha$ -(Mg,Fe)<sub>2</sub>SiO<sub>4</sub> and  $\gamma$ -(Mg,Fe)<sub>2</sub>SiO<sub>4</sub> in the sample S2 position at pressures of 7.5–11.2 GPa (Fig. 3), and the SEM analyses show the coexistence of Mg- and Fe-rich olivine solid solutions in the same sample position (Fig. 2b). Considering previous studies (Akimoto and Fujisawa 1968; Frost

**Fig. 3** XRD patterns of the run products obtained after quench. The blue, red, and green numbers indicate the Miller indexes of olivine, ahrensite, and wadsleyite, respectively. The (110) peak from the molybdenum disk is marked with a purple asterisk. The sample position, composition of the starting material, and run number are indicated on the left side



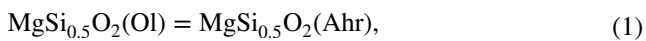
2003), these Mg-rich and Fe-rich phases should be olivine and ahrensite, respectively (Table S1).

The compositions of the coexisting olivine and ahrensite based on the EPMA analyses are listed in Tables 1 and S2. With increasing pressure from 7.5 to 11.2 GPa, the  $Fe_2SiO_4$  component decreases from 0.705 to 0.227 in olivine and from 0.878 to 0.482 in ahrensite.

Coexisting olivine and wadsleyite were found at 12.5 GPa and 1748.0 K in the S1 sample position. The  $Fe_2SiO_4$  contents were determined as 0.126 and 0.200 in olivine and wadsleyite, respectively.

### Thermodynamic approach

The exchange of Fe and Mg between olivine and ahrensite can be expressed by the following reactions:



where Ol and Ahr represent olivine and ahrensite, respectively.

The changes of Gibbs free energy for reactions (1) and (2),  $\Delta G_{MgSi_{0.5}O_2}(P, T)$  and  $\Delta G_{FeSi_{0.5}O_2}(P, T)$ , respectively, are expressed as:

$$\begin{aligned} \Delta G_{MgSi_{0.5}O_2}(P, T) &= \Delta G_{MgSi_{0.5}O_2}^0 \\ &+ \int_0^P \Delta V_{MgSi_{0.5}O_2}(P, T) + RT \ln \frac{a_{MgSi_{0.5}O_2}^{Ahr}}{a_{MgSi_{0.5}O_2}^{Ol}}, \end{aligned} \tag{3}$$

$$\begin{aligned} \Delta G_{FeSi_{0.5}O_2}(P, T) &= \Delta G_{FeSi_{0.5}O_2}^0 \\ &+ \int_0^P \Delta V_{FeSi_{0.5}O_2}(P, T) + RT \ln \frac{a_{FeSi_{0.5}O_2}^{Ahr}}{a_{FeSi_{0.5}O_2}^{Ol}}, \end{aligned} \tag{4}$$

where  $T$  is the absolute temperature,  $\Delta G_{MgSi_{0.5}O_2}^0$  and  $\Delta G_{FeSi_{0.5}O_2}^0$  are the Gibbs free energy changes in reactions (1) and (2) at 1 atm and 1740 K,  $\Delta V_{MgSi_{0.5}O_2}(P, T)$  and  $\Delta V_{FeSi_{0.5}O_2}$  are the volume changes at a pressure of  $P$  and temperature of  $T$ , and  $a_M^N$  is the activity of component  $M$  ( $MgSi_{0.5}O_2$  or  $FeSi_{0.5}O_2$ ) in phase  $N$ . The temperature is fixed at 1740 K in the calculation.

The  $a_M^N$  term is expressed as:

**Table 2** Covariance matrix of the parameters ( $\Delta G_{\text{MgSi}_{0.5}\text{O}_2}^0$ ,  $\Delta G_{\text{FeSi}_{0.5}\text{O}_2}^0$ ,  $W^{\text{Ol}}$ , and  $W^{\text{Ahr}}$ , in kJ/mol) in least square fitting

$(\Delta G_{\text{MgSi}_{0.5}\text{O}_2}^0, W^{\text{Ol}}, \text{ and } W^{\text{Ahr}} \text{ in Eq. (7)})$			
	$\Delta G_{\text{MgSi}_{0.5}\text{O}_2}^0$	$W^{\text{Ol}}$	$W^{\text{Ahr}}$
$\Delta G_{\text{MgSi}_{0.5}\text{O}_2}^0$	0.8	-3.2	-3.5
$W^{\text{Ol}}$	-3.2	14.1	16.3
$W^{\text{Ahr}}$	-3.5	16.3	19.7
$(\Delta G_{\text{FeSi}_{0.5}\text{O}_2}^0, W^{\text{Ol}}, \text{ and } W^{\text{Ahr}} \text{ in Eq. (8)})$			
	$\Delta G_{\text{FeSi}_{0.5}\text{O}_2}^0$	$W^{\text{Ol}}$	$W^{\text{Ahr}}$
$\Delta G_{\text{FeSi}_{0.5}\text{O}_2}^0$	0.1	0.3	0.2
$W^{\text{Ol}}$	0.3	7.2	3.5
$W^{\text{Ahr}}$	0.2	3.5	1.8

$$a_M^N = X_M^N \times \gamma_M^N \quad (5)$$

where  $X_M^N$  is the concentration and  $\gamma_M^N$  is the activity coefficient of component  $M$  in phase  $N$ .

Based on the symmetric regular solution model, the activity coefficient can be written as:

$$RT \ln \gamma_M^N = W^N (1 - X_M^N)^2, \quad (6)$$

where  $W^N$  is the Margules interaction parameter that describes the interaction energy between Fe and Mg in the solid solutions.

Equations (3)–(6) lead to:

$$\Delta G_{\text{MgSi}_{0.5}\text{O}_2}(P, T) = \Delta G_{\text{MgSi}_{0.5}\text{O}_2}^0 + \int_0^P \Delta V_{\text{MgSi}_{0.5}\text{O}_2}(P, T) + RT \ln \frac{X_{\text{MgSi}_{0.5}\text{O}_2}^{\text{Ahr}}}{X_{\text{MgSi}_{0.5}\text{O}_2}^{\text{Ol}}} + W^{\text{Ahr}} (X_{\text{FeSi}_{0.5}\text{O}_2}^{\text{Ahr}})^2 - W^{\text{Ol}} (X_{\text{FeSi}_{0.5}\text{O}_2}^{\text{Ol}})^2, \quad (7)$$

$$\Delta G_{\text{FeSi}_{0.5}\text{O}_2}(P, T) = \Delta G_{\text{FeSi}_{0.5}\text{O}_2}^0 + \int_0^P \Delta V_{\text{FeSi}_{0.5}\text{O}_2}(P, T) + RT \ln \frac{X_{\text{FeSi}_{0.5}\text{O}_2}^{\text{Ahr}}}{X_{\text{FeSi}_{0.5}\text{O}_2}^{\text{Ol}}} + W^{\text{Ahr}} (1 - X_{\text{FeSi}_{0.5}\text{O}_2}^{\text{Ahr}})^2 - W^{\text{Ol}} (1 - X_{\text{FeSi}_{0.5}\text{O}_2}^{\text{Ol}})^2. \quad (8)$$

The molar volumes of the  $\text{MgSi}_{0.5}\text{O}_2$  and  $\text{FeSi}_{0.5}\text{O}_2$  endmembers of forsterite–fayalite and ringwoodite–ahrensite have been previously reported as functions of pressure and temperature (Jacobs et al. 2001; Katsura et al. 2004, 2009). They were recalculated for 1740 K and various pressure conditions using their reported parameters for thermal coefficients and high-temperature Birch–Murnaghan equations of state (Table 1). The  $\Delta V_{\text{MgSi}_{0.5}\text{O}_2}$  and  $\Delta V_{\text{FeSi}_{0.5}\text{O}_2}$  values at 1740 K are thus obtained from the molar volumes of the endmembers.

Under equilibrium conditions, both  $\Delta G_{\text{MgSi}_{0.5}\text{O}_2}$  and  $\Delta G_{\text{FeSi}_{0.5}\text{O}_2}$  equal 0. With these constraints,  $\Delta G_{\text{MgSi}_{0.5}\text{O}_2}^0$ ,  $\Delta G_{\text{FeSi}_{0.5}\text{O}_2}^0$ ,  $W^{\text{Ol}}$ , and  $W^{\text{Ahr}}$  were obtained by simultaneous least square fitting of the experimental data to Eqs. (7) and

(8):  $\Delta G_{\text{MgSi}_{0.5}\text{O}_2}^0 = 28.4$  kJ/mol;  $\Delta G_{\text{FeSi}_{0.5}\text{O}_2}^0 = 14.5$  kJ/mol;  $W^{\text{Ol}} = 1.7$  kJ/mol; and  $W^{\text{Ahr}} = 1.5$  kJ/mol. Note that the  $W^{\text{Ol}}$  and  $W^{\text{Ahr}}$  are strongly correlated in least square fitting, therefore, it is not appreciate to report an individual uncertainty each parameter, instead, the co-variance matrix is shown in Table 2 for Eqs. (7) and (8), which shows the correlation of the fitting parameters.

By inputting a pressure value, the compositions of olivine and ahrensite ( $X_{\text{FeSi}_{0.5}\text{O}_2}^{\text{Ol}}$ ,  $X_{\text{FeSi}_{0.5}\text{O}_2}^{\text{Ahr}}$ ) are calculated from Eqs. (7) and (8) and the curves of the olivine–ahrensite loop at 1740 K are obtained at various pressures (Fig. 4).

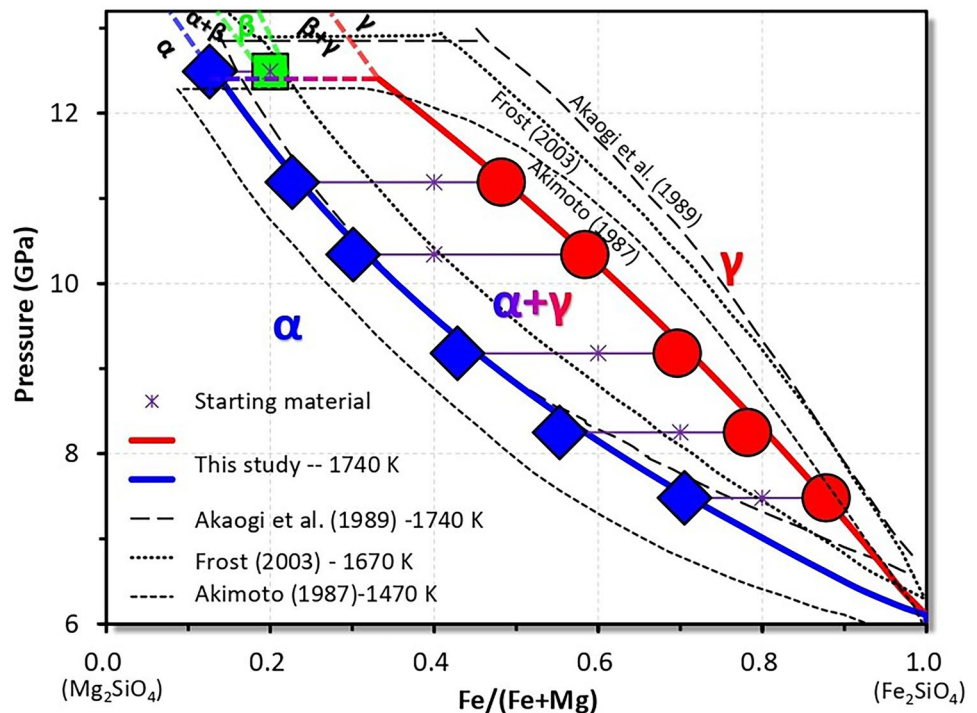
A user-friendly software named “olivine–ahrensite loop

calculation tool” was developed to quantitatively determine pressure and temperature conditions from the compositions of coexisting olivine and ahrensite. The software instructions are provided in the supplementary material.

## Comparison with previous results

A comparison of our results with previously published data is shown in Fig. 4. The binary loop at 1470 K (Akimoto 1987) was constructed based only on high-pressure experimental data, whereas the loops at 1670–1740 K were calculated thermodynamically using data obtained either from high-pressure experiments (Frost 2003) or calorimetric measurements at ambient pressure (Akaogi et al. 1989). We

**Fig. 4** Comparison between olivine–ahrensite loop determined in our study with previously published ones (Akaogi et al. 1989; Akimoto 1987; Frost 2003). The blue, red, and green symbols are the compositions of olivine, ahrensite, and wadsleyite, respectively, from EPMA analysis. Symbol sizes are larger than pressure determination errors. The solid curves show the results of the thermodynamic calculation using our data at 1740 K. The 1473 and 1873 K data from Akaogi et al. (1989) are recalculated to 1740 K, whereas the temperature conditions of Akimoto (1987) and Frost (2003) are 1470 and 1670 K, respectively.  $\alpha$ :  $\alpha$ -(Mg,Fe)<sub>2</sub>SiO<sub>4</sub> olivine.  $\beta$ :  $\beta$ -(Mg,Fe)<sub>2</sub>SiO<sub>4</sub> wadsleyite.  $\gamma$ :  $\gamma$ -(Mg,Fe)<sub>2</sub>SiO<sub>4</sub> ahrensite



recalculated an olivine–ahrensite loop from Akaogi et al. (1989) at 1740 K based on their 1473 and 1873 K data. Our determined olivine–ahrensite loop is shifted to the Mg<sub>2</sub>SiO<sub>4</sub> side compared with the loop reported by Frost (2003) and located within the loops defined by Akaogi et al. (1989) and Akimoto (1987) (Fig. 4). The widths of the loops obtained in our study and by Frost (2003) are similar and narrower than those by Akaogi et al. (1989) and Akimoto (1987).

The phase boundary between the fields of coexisting olivine/ahrensite and olivine/wadsleyite was determined between 11.2 and 12.5 GPa. Due to the topology of the phase diagram and the rules of metastable extensions (Frost 2003), the olivine edge of olivine–wadsleyite loop has a less steep  $\Delta P/\Delta \#Mg$  slope than that of the olivine–ahrensite loop. The boundary between the olivine–ahrensite and olivine–wadsleyite loops should, therefore, be located at a pressure slightly below 12.5 GPa because the composition of olivine coexisting with wadsleyite ((Mg<sub>0.874</sub>Fe<sub>0.126</sub>)<sub>2</sub>SiO<sub>4</sub>) at 12.5 GPa and 1748.0 K is similar to that coexisting with ahrensite by the thermochemical calculation ((Mg<sub>0.867</sub>Fe<sub>0.133</sub>)<sub>2</sub>SiO<sub>4</sub>). If the boundary between the olivine–ahrensite and olivine–wadsleyite loops is located at a pressure significantly below 12.5 GPa, the olivine in coexistence with wadsleyite should be much more magnesian. In previous studies, this boundary was considered to be at 12.8 GPa (Akaogi et al. 1989; Frost 2003) and 12.2 GPa (Akimoto 1987).

In general, our data are in good agreement with Frost (2003). Figure 4 in Frost (2003) shows that his experimentally determined data points of olivine and ahrensite coexistence are located at lower pressures than those predicted

by his thermochemical calculation, which suggests that the olivine–ahrensite loop should be located at lower pressure. Our results are thus consistent with the Frost (2003) experimental data. As shown above, the discrepancy between the experimental data and calculated binary loop in Frost (2003) can be explained by uncertainties in the thermochemical calculation. Frost (2003) confirmed the chemical equilibrium of the partition data by conducting normal and reversal runs, thus the agreement in composition between our study and Frost (2003) suggests that our samples also reached chemical equilibrium.

The olivine–ahrensite loop at 1470 K shown in Akimoto (1987) is considerably wider than that determined in our study at 1740 K (Fig. 4). However, judging from the original experimental data (Akimoto 1987), one can suggest that the loop should be much narrower. The data points in Akimoto (1987) were also obtained by XRD of the entire recovered samples. This method does not provide sufficient data accuracy in comparison with compositional analysis, nor can it confirm the chemical equilibrium of the system. The data in Akimoto (1987) were also obtained at a lower temperature. There are, therefore, several possible explanations for the discrepancy between the loop widths.

The calculated olivine–ahrensite loop from Akaogi et al. (1989) is also much wider than that determined in our study, which can be explained by the different Margules interaction parameters. Frost (2003) calculated the loop using the procedure as in Akaogi et al. (1989), but applied different interaction parameters and obtained a narrower loop, which is similar to the loop determined in this study.

**Table 3** Comparison of experimental pressures and calculated pressures from the fitted olivine–ahrensite loop

Run. No.	T (K) after correction	P (GPa) after correction	P (GPa) calculated at 1740 K	$ \Delta P $ (GPa)
HH310	1744.6 (1.1)	11.19 (17)	11.27 (8)	0.08
HH300	1743.4 (2.4)	10.34 (11)	10.40 (2)	0.06
HH311	1737.9 (1.0)	9.18 (14)	9.29 (8)	0.11
HH312	1735.3 (9)	8.25 (13)	8.39 (9)	0.14
HH314	1732.6 (6)	7.48 (13)	7.41 (1)	0.07

$|\Delta P|$  was calculated by subtracting the pressure determined by the MgO unit cell volumes ( $P$  after correction) from that determined by the Mg# of olivine and ahrensite ( $P$  calculated at 1740 K). We provide the absolute value of this difference

### Multi-anvil press calibration

The obtained results can be applied for in-house pressure calibration of multi-anvil apparatuses at high temperature. In principle, one olivine sample that transforms to olivine and ahrensite at 1740 K is sufficient to determine the pressure in the range of 6.5–12.0 GPa. However, because it can be difficult to select a single sample that will fall within the loop under experimental conditions, we propose to place several olivine samples in one run. For example, if the expected pressure is around 10 GPa, placing Fo40, Fo50 and Fo60 disks should ensure successful pressure determination. After the experiment, the compositions of the coexisting olivine and ahrensite in the run product should be accurately measured by EPMA. The compositions (Mg#) of both phases should correspond to the same pressure, thus confirming their chemical equilibrium and providing a precise pressure determination. The current version of the software allows calculation of the olivine–ahrensite loops at temperatures from 1600 to 1900 K, but the most reliable results are provided at  $1740 \pm 10$  K because experimental data are presently lacking at other temperatures. We, therefore, strongly recommend conducting such calibration experiments at 1740 K. To confirm the reliability of the proposed method, we recalculated pressure values for each experimental point using the olivine–ahrensite loop calculation tool software at a fixed temperature of 1740 K and compared the results with values obtained during the experiments (Table 3). The observed discrepancies are within the pressure determination errors ( $<0.15$  GPa).

The proposed method has essential advantages in comparison with conventional in-house multi-anvil press calibration techniques at high temperature, such as the quartz–coesite–stishovite transitions in  $\text{SiO}_2$  (Mirwald and Massonne 1980; Ono et al. 2017) or fayalite–ahrensite transition in pure  $\text{Fe}_2\text{SiO}_4$  (Yagi et al. 1987). These conventional techniques require several experimental runs with different press loads to bracket the phase transitions, whereas olivine–ahrensite coexistence from olivine solid solution provides the pressure determination in a single run. Olivine–ahrensite coexistence also allows pressure

determination between 6.5 and 12.0 GPa, whereas other high-temperature calibrations are limited to the exact transition pressure at a given temperature. Olivine samples can be loaded in the corner of the sample chamber to estimate the sample pressure in any experimental run at 1740 K and 6.5–12.0 GPa. Precise pressure determinations at temperatures other from 1740 K require further experimental studies to determine the olivine–ahrensite loop at such temperatures.

### Determination of shock parameters

Olivine and ahrensite (ringwoodite) are common minerals in shocked meteorites (e.g. Acosta-Maeda et al. 2013; Baziotis et al. 2018; Feng et al. 2011; Ma et al. 2016; Miyahara et al. 2010; Pittarello et al. 2015; Sharp et al. 2019; Walton and McCarthy 2017). It is expected that shock conditions can be estimated using the compositions of coexisting olivine and ahrensite based on the phase diagram of the olivine–ahrensite transition. More concretely, the Fe–Mg partition coefficients between olivine and ahrensite should indicate shock temperatures. Shock pressures can be obtained using these temperatures and the Mg# values of these minerals. Unfortunately, shock temperatures cannot be estimated solely based on the present results because we determined the phase relations only at a single temperature of 1740 K. We, therefore, include literature data related to the temperature dependence to temporarily attempt to estimate shock pressures and temperatures using the olivine–ahrensite loop calculation tool software developed here. However, these estimates will be revised after determining the phase relations at different temperatures in our future studies.

We attempted to estimate shock parameters of several meteorites based on the published data regarding the compositions of coexisting olivine and ahrensite (ringwoodite) in Martian meteorites and chondrites (Table 4). Our estimations are based on the assumption that both olivine and ahrensite are in equilibrium, which is confirmed by the difference in the compositions of these minerals. If the transformation occurs out of equilibrium, by overstepping the equilibrium phase boundary in pressure, the same transformation

**Table 4** Compositions of coexisting olivine and ringwoodite (ahrensite) in meteorites

Meteorite	Type	Reference	Olivine	Ahrensite	T, K	P, GPa
Tissint	Martian (shergottite)	Ma et al. (2016)	Fe <sub>0.64</sub> Fa <sub>0.36</sub>	Rw <sub>0.46</sub> Ahr <sub>0.54</sub>	1900	10.5 (7)
NWA 8159	Martian (aug. basalt)	Sharp et al. (2019)	Fe <sub>0.34</sub> Fa <sub>0.66</sub>	Rw <sub>0.26</sub> Ahr <sub>0.74</sub>	1900	8.4 (8)
Taiban	L5	Acosta-Maeda et al. (2013)	Fe <sub>0.92</sub> Fa <sub>0.08</sub>	Rw <sub>0.73</sub> Ahr <sub>0.27</sub>	1600	> 12.4 (8)
Dhofar 1970	L5	Walton and McCarthy (2017)	Fe <sub>0.86</sub> Fa <sub>0.14</sub>	Rw <sub>0.54</sub> Ahr <sub>0.46</sub>	1600	11.7 (5)
Asuka-09584	L6	Pittarello et al. (2015)	Fe <sub>0.83</sub> Fa <sub>0.17</sub>	Rw <sub>0.58</sub> Ahr <sub>0.42</sub>	1600	11.6
Château-Renard	L6	Baziotis et al. (2018)	Fe <sub>0.80</sub> Fa <sub>0.20</sub>	Rw <sub>0.55</sub> Ahr <sub>0.45</sub>	1700	11.5

Olivine and ringwoodite compositions are given as forsterite (Mg<sub>2</sub>SiO<sub>4</sub>)–fayalite (Fe<sub>2</sub>SiO<sub>4</sub>) and ringwoodite (Mg<sub>2</sub>SiO<sub>4</sub>)–ahrensite (Fe<sub>2</sub>SiO<sub>4</sub>) solid solutions

Aug. basalt augite basalt

should occur without a change in composition (Sharp and DeCarli 2006). Nevertheless, equilibrium in shock processes remains a controversial issue, because in the same meteorite both low-pressure parageneses and high-pressure parageneses can occur. Estimated shock temperature and pressures of Martian meteorites Tissint (Ma et al. 2016) and NWA 8159 (Sharp et al. 2019) are 1900 K and 8.4 (8) and 10.5 (7) GPa, respectively. Shock parameters of L5-type chondrites Taiban (Acosta-Maeda et al. 2013) and Dhofar 1970 (Walton and McCarthy 2017) were estimated as 1600 K and > 12.4 (8) and 11.7 (5) GPa, respectively. Because these estimates yield large errors, we suppose that these Martian meteorites and L5-type chondrites should have been impacted at > 1900 K and < 1200 K, respectively. Shock conditions of L6-type chondrites Asuka-09584 (Pittarello et al. 2015) and Château-Renard (Baziotis et al. 2018) were estimated as 1600 K and 11.6 GPa and 1700 K and 11.5 GPa, respectively. Because these temperatures are relatively close to 1740 K, we suggest that these parameters are rather accurate. It is also important to note that these parameters do not indicate peak shock conditions because both meteorites contain higher-pressure phases, such as bridgmanite (Baziotis et al. 2018) and maskelynite (Pittarello et al. 2015). However, obtained temperature and pressure parameters can be useful for the construction of the pressure–temperature paths after passing the peak pressure.

## Conclusions

The binary loop of the olivine–ahrensite transition in the (Mg,Fe)<sub>2</sub>SiO<sub>4</sub> system at a temperature of 1740 K in the pressure range of 7.5–11.2 GPa was determined using a multi-anvil apparatus combined with in situ X-ray diffraction. The Fe<sub>2</sub>SiO<sub>4</sub> components in olivine and ahrensite decrease with increasing pressure from 0.705 and 0.878 at 7.5 GPa to 0.227 and 0.482 at 11.2 GPa, respectively. A convenient software was developed to calculate pressure from compositions of coexisting olivine and ahrensite.

This software was tested by comparing the obtained pressures with those determined using MgO unit cell volumes. The present phase relation can be used for precise in-house multi-anvil press calibration at high temperature in the pressure range from 6.5 to 12.0 GPa. This software can also be used to estimate shock conditions of L6-type chondrites Asuka-09584 and Château-Renard meteorites as 1600 K, 11.6 GPa and 1700 K, 11.5 GPa, respectively.

**Supplementary Information** The online version contains supplementary material available at <https://doi.org/10.1007/s00410-021-01829-x>.

**Acknowledgements** We appreciate H. Fischer, S. Übelhack, R. Njul, U. Trenz, and S. Linhardt at the Bayerisches Geoinstitut and S. Sonntag at DESY for their technical assistance and E. Posner for English correction of the manuscript. We thank D. Frost and M. Akaogi for helpful discussion.

**Author contributions** DB and TI prepared the starting materials and wrote “Sample preparation” section. KN prepared the cell assembly details. NP conducted SEM and EPMA analyses and wrote “Sample analyses” section. HF conducted thermodynamic calculations, wrote “Thermodynamic approach” section, and prepared the olivine–ahrensite loop calculation tool software and its instructions. SB and RF assisted in conducting experiments. TK directed the project and wrote “Introduction” section. AC conducted the experiments, wrote the remaining sections, and prepared manuscript for submission. All authors commented on the manuscript.

**Funding** Open Access funding enabled and organized by Projekt DEAL. This work was funded by a research project approved by the Federal Ministry of Education and Research (BMBF) (05K16WC2) and the European Research Council (ERC) under the European Union’s Horizon 2020 research and innovation program (Proposal No. 787 527) to T. Katsura. The synchrotron X-ray diffraction experiments were performed at the PETRA III beamline P61B at DESY (Hamburg, Germany), a member of the Helmholtz Association HGF.

**Data availability** All data and material used and discussed in the text are included as Figures and Tables in the main text or in the Electronic Supplementary Material.

**Code availability** The olivine–ahrensite loop calculation tool software was used to calculating and illustrate Fig. 4. The software and its instructions are attached to the Supplementary Information.

## Declarations

**Conflict of interest** The authors declare that they have no conflict of interest.

**Open Access** This article is licensed under a Creative Commons Attribution 4.0 International License, which permits use, sharing, adaptation, distribution and reproduction in any medium or format, as long as you give appropriate credit to the original author(s) and the source, provide a link to the Creative Commons licence, and indicate if changes were made. The images or other third party material in this article are included in the article's Creative Commons licence, unless indicated otherwise in a credit line to the material. If material is not included in the article's Creative Commons licence and your intended use is not permitted by statutory regulation or exceeds the permitted use, you will need to obtain permission directly from the copyright holder. To view a copy of this licence, visit <http://creativecommons.org/licenses/by/4.0/>.

## References

- Acosta-Maeda TE, Scott ER, Sharma SK, Misra AK (2013) The pressures and temperatures of meteorite impact: evidence from micro-Raman mapping of mineral phases in the strongly shocked Taiban ordinary chondrite. *Am Miner* 98(5–6):859–869
- Akaogi M, Ito E, Navrotsky A (1989) Olivine-modified spinel-spinel transitions in the system  $Mg_2SiO_4$ - $Fe_2SiO_4$ : calorimetric measurements, thermochemical calculation, and geophysical application. *J Geophys Res Solid Earth* 94(B11):15671–15685
- Akimoto SI (1987) High-pressure research in geophysics: past, present and future. *High Press Res Miner Phys A Vol Honor Syun Iti Akimoto* 39:1–13
- Akimoto SI, Fujisawa H (1968) Olivine-spinel solid solution equilibria in the system  $Mg_2SiO_4$ - $Fe_2SiO_4$ . *J Geophys Res* 73(4):1467–1479
- Armstrong JT (1991) Quantitative elemental analysis of individual microparticles with electron beam instruments. In: Heinrich Kfj, Newbury DE (eds) *Electron probe quantitation*. Plenum Press, New York, pp 261–315
- Baziotis I, Asimow PD, Hu J, Ferrière L, Ma C, Cernok A, Anand M, Topa D (2018) High pressure minerals in the Château-Renard (L6) ordinary chondrite: implications for collisions on its parent body. *Sci Rep* 8(1):1–16
- Binns R, Davis R, Reed S (1969) Ringwoodite, natural ( $Mg, Fe_2SiO_4$  spinel) in the Tenham meteorite. *Nature* 221(5184):943–944
- Feng L, Lin Y, Hu S, Xu L, Miao B (2011) Estimating compositions of natural ringwoodite in the heavily shocked Grove Mountains 052049 meteorite from Raman spectra. *Am Miner* 96(10):1480–1489
- Frost DJ (2003) The structure and sharpness of ( $Mg, Fe$ ) $_2SiO_4$  phase transformations in the transition zone. *Earth Planet Sci Lett* 216(3):313–328
- Ishii T, Huang R, Fei H, Koemets I, Liu Z, Maeda F, Yuan L, Wang L, Druzhbin D, Yamamoto T (2018) Complete agreement of the post-spinel transition with the 660-km seismic discontinuity. *Sci Rep* 8(1):1–6
- Ishii T, Huang R, Myhill R, Fei H, Koemets I, Liu Z, Maeda F, Yuan L, Wang L, Druzhbin D (2019) Sharp 660-km discontinuity controlled by extremely narrow binary post-spinel transition. *Nat Geosci* 12(10):869–872
- Jacobs MH, de Jong BH, Onk HA (2001) The Gibbs energy formulation of  $\alpha$ ,  $\gamma$ , and liquid  $Fe_2SiO_4$  using Grover, Getting, and Kennedy's empirical relation between volume and bulk modulus. *Geochim Cosmochim Acta* 65(22):4231–4242
- Katsura T, Yokoshi S, Song M, Kawabe K, Tsujimura T, Kubo A, Ito E, Tange Y, Tomioka N, Saito K (2004) Thermal expansion of  $Mg_2SiO_4$  ringwoodite at high pressures. *J Geophys Res Solid Earth* 109(B12). <https://doi.org/10.1029/2004JB003094>
- Katsura T, Shatskiy A, Manthilake MGM, Zhai S, Fukui H, Yamazaki D, Matsuzaki T, Yoneda A, Ito E, Kuwata A (2009) Thermal expansion of forsterite at high pressures determined by *in situ* X-ray diffraction: the adiabatic geotherm in the upper mantle. *Phys Earth Planet Inter* 174(1–4):86–92
- Khan A, Liebske C, Rozel A, Rivoldini A, Nimmo F, Connolly J, Plesa AC, Giardini D (2018) A geophysical perspective on the bulk composition of Mars. *J Geophys Res Planets* 123(2):575–611
- Ma C, Tschauner O, Beckett JR, Liu Y, Rossman GR, Sinogeikin SV, Smith JS, Taylor LA (2016) Ahrensite,  $\gamma$ - $Fe_2SiO_4$ , a new shock-metamorphic mineral from the Tissint meteorite: implications for the Tissint shock event on Mars. *Geochim Cosmochim Acta* 184:240–256
- McDonough WF, Sun S-S (1995) The composition of the Earth. *Chem Geol* 120(3–4):223–253
- Mirwald PW, Massonne HJ (1980) The low-high quartz and quartz-coesite transition to 40 kbar between 600° and 1600°C and some reconnaissance data on the effect of  $NaAlO_2$  component on the low quartz-coesite transition. *J Geophys Res Solid Earth* 85(B12):6983–6990
- Miyahara M, Ohtani E, Kimura M, El Goresy A, Ozawa S, Nagase T, Nishijima M, Hiraga K (2010) Coherent and subsequent incoherent ringwoodite growth in olivine of shocked L6 chondrites. *Earth Planet Sci Lett* 295(1–2):321–327
- Nishida K, Xie L, Kim EJ, Katsura T (2020) A strip-type boron-doped diamond heater synthesized by chemical vapor deposition for large-volume presses. *Rev Sci Instrum* 91(9):095108
- Nishihara Y, Doi S, Kakizawa S, Higo Y, Tange Y (2020) Effect of pressure on temperature measurements using WRe thermocouple and its geophysical impact. *Phys Earth Planet Inter* 298:106348
- Ono S, Kikegawa T, Higo Y, Tange Y (2017) Precise determination of the phase boundary between coesite and stishovite in  $SiO_2$ . *Phys Earth Planet Inter* 264:1–6
- Pittarello L, Ji G, Yamaguchi A, Schryvers D, Debaille V, Claeys P (2015) From olivine to ringwoodite: a TEM study of a complex process. *Meteorit Planet Sci* 50(5):944–957
- Ringwood A (1958) The constitution of the mantle—II: further data on the olivine-spinel transition. *Geochim Cosmochim Acta* 15(1–2):18–29
- Sanchez JA, Reddy V, Kelley MS, Cloutis EA, Bottke WF, Nesvorný D, Lucas MP, Hardersen PS, Gaffey MJ, Abell PA (2014) Olivine-dominated asteroids: mineralogy and origin. *Icarus* 228:288–300
- Sharp TG, DeCarli PS (2006) Shock effects in meteorites. *Meteor Early Solar Syst II* 943:653–677
- Sharp TG, Walton EL, Hu J, Agee C (2019) Shock conditions recorded in NWA 8159 martian augite basalt with implications for the impact cratering history on Mars. *Geochim Cosmochim Acta* 246:197–212
- Tange Y, Nishihara Y, Tsuchiya T (2009) Unified analyses for P-V-T equation of state of  $MgO$ : a solution for pressure-scale problems in high P-T experiments. *J Geophys Res Solid Earth* 114(B3). <https://doi.org/10.1029/2008JB005813>
- Walton EL, McCarthy S (2017) Mechanisms of ringwoodite formation in shocked meteorites: evidence from L5 chondrite Dhofar 1970. *Meteorit Planet Sci* 52(4):762–776
- Yagi T, Akaogi M, Shimomura O, Suzuki T, Akimoto SI (1987) *In situ* observation of the olivine-spinel phase transformation in  $Fe_2SiO_4$  using synchrotron radiation. *J Geophys Res Solid Earth* 92(B7):6207–6213

**Publisher's Note** Springer Nature remains neutral with regard to jurisdictional claims in published maps and institutional affiliations.